
State-to-state reaction dynamics in crossed supersonic jets: threshold evidence for non-adiabatic channels in $F + H_2$

Sergey A. Nizkorodov, Warren W. Harper and David J. Nesbitt*

*JILA, University of Colorado and National Institute of Standards and Technology and
Department of Chemistry and Biochemistry, University of Colorado, Boulder, CO
80309-0440, USA*

Received 9th March 1999

The reaction of $F + n-H_2$ to form $HF(v,J) + H$ is studied in a crossed jet apparatus under single collision conditions, using high-resolution direct absorption spectroscopy to probe the nascent rotational HF distributions. The J -dependent reactive cross-sections into $HF(v = 3,J)$ are investigated over a range of center-of-mass collision energies well below the $1.9 \text{ kcal mol}^{-1}$ barrier for *adiabatic* chemical reactions with *ground state* $F(^2P_{3/2})$ atoms. The energy dependent reaction cross-sections decrease much more slowly with E_{com} than predicted by exact quantum calculations on the *adiabatic* $F(^2P_{3/2}) + H_2$ surface (K. Stark and H. Werner, *J. Chem. Phys.*, 1996, **104**, 6515). In addition, product states in the $HF(v = 3)$ manifold are observed that are energetically accessible only to the *excited spin-orbit* state $F^*(P_{1/2}) + H_2(j = 0,1)$ channel. These observations strongly suggest that *non-adiabatic* reactions with spin-orbit excited $F^*(P_{1/2})$ contribute significantly in the near threshold region, in good agreement with recent calculations by M. Alexander, H. Werner and D. Manolopoulos (*J. Chem. Phys.*, 1998, **109**, 5710). Finally, the feasibility of high-resolution IR laser Dopplerimetry on the nascent products is illustrated on collision free $HF(v,J)$ distributions formed from reactions of $F + CH_4$.

I Introduction

It has been long recognized that chemistry in typical gas-phase environments ranging from the Earth's atmosphere to the interstellar medium is driven primarily by reactions involving transient species, such as free radicals and molecular ions, as these reactions are frequently characterized by high rates and low activation energies. Though the scientific community has made substantial progress towards the dynamics of such reactions in recent years, our understanding of elementary chemical processes is far from complete. Even the prototypic $F + H_2$ reaction system, which has been under intense scientific scrutiny for several decades,¹⁻⁴ still has several key issues to be resolved. As one example of central relevance to the present work, the importance of F/F^* electronic spin-orbit excitation, or alternatively stated, the role of *adiabatic* vs. *non-adiabatic* reaction pathways in chemical reactions, remains an outstanding and yet crucial question in reaction rate theory.⁵ The very fundamental level of these questions underscores the need for further experimental and theoretical efforts to elucidate "simple" atom abstraction dynamics at the state-to-state level.

Recently, the dynamics of the $F + H_2$ reaction has been investigated in our laboratory with crossed supersonic jets.⁶ The full nascent state distribution of the HF products has been obtained

Faraday Discuss., 1999, **113**, 107-117 **107**

at $E_{\text{com}} = 2.4(6)$ kcal mol⁻¹ under single collision conditions using direct infrared absorption high-resolution spectroscopy. These direct absorption studies have become experimentally feasible due to a combination of near shot-noise limited absorption sensitivity and an efficient source of atomic free radicals developed in our group.⁶ The source utilizes an electrical discharge struck in the jet stagnation region to generate high radical densities followed by supersonic expansion. Spectroscopic measurements in this laboratory show that the radical number densities of 10¹⁵ cm⁻³ at the orifice can be routinely achieved. In the present work, we report results at center-of-mass collision energies substantially *below* the 1.9 kcal mol⁻¹ reaction barrier theoretically predicted^{3,7} for the lowest *adiabatic* F(²P_{3/2}) + H₂ potential energy surface (PES). This choice of center-of-mass collision energy greatly suppresses reactive encounters on the *ground spin-orbit* adiabatic surface, and thereby selectively enhancing the importance of non-adiabatic pathways with *spin-orbit excited* F*(²P_{1/2}) atoms. Additionally, we demonstrate the experimental feasibility of obtaining state-to-state *differential cross-section* information from high-resolution IR laser Dopplerimetry, as briefly tested by application to the F + CH₄ reaction.

The F + H₂ reaction system represents one of the quintessential paradigms of chemical reaction dynamics. As a consequence, the body of existing experimental and theoretical knowledge is immense; the interested reader is referred to an excellent review by Manolopoulos³ for a more detailed discussion and further references. The key points most relevant to the present study can be summarized as follows. (i) The high reaction exothermicity ($\Delta E = 32.001(14)$ kcal mol⁻¹ for F(²P_{3/2}) + H₂($j = 0$) → HF($v = 0, J = 0$) + H) is primarily released into a vibrationally inverted HF($v \leq 3$) product distribution, which has been characterized by a number of experimental methods at increasing levels of quantum state resolution.^{6,8-11} (ii) The unpaired electron in the F results in multiple potential energy surfaces, which asymptotically correlate with either the lower F(²P_{3/2}) or upper F*(²P_{1/2}) spin-orbit states. Most importantly, reactions initiated on the surfaces other than the *lowest* PES are repulsive in the transition state region and therefore predicted to be forbidden in the Born-Oppenheimer (*i.e.*, purely adiabatic) approximation.^{12,13} Though theory claims that this restriction can be lifted by means of weak non-adiabatic interactions, no experiments to date have been able to unambiguously confirm the presence of the F* + H₂ reaction channel.³ (iii) The relevant potential energy surfaces have been calculated by *ab initio* methods by Stark and Werner (SW) with the stated global accuracy of better than ± 0.2 kcal mol⁻¹,⁷ and later extended to include the spin-orbit interaction by Hartke and Werner (SHW).¹⁴ (iv) Classical trajectory and full quantum-mechanical calculations performed on the lowest adiabatic SW/SHW PES can qualitatively reproduce much of the prevailing experimental data on the F + H₂ reaction, including differential cross-sections,¹⁵⁻¹⁸ thermal rate constants,^{19,20} and nascent HF product state distributions.⁶

The major focus of this work is to examine the possibility of *non-adiabatic* channels in this most basic and extraordinarily well studied of chemical reactions. The essential idea is schematically summarized in Fig. 1. The radical source generates both ground (F) and spin-orbit excited (F*) atoms in the high pressure discharge region (most likely in a near statistical $\approx 4 : 2$ ratio), which are inefficiently cooled in the subsequent supersonic expansion. These F/F* atoms collide with jet cooled H₂ molecules at a center-of-mass collision energy dictated by the jet velocities, which are measured by direct time-of-flight and/or high resolution IR Dopplerimetry on each jet. By operating at center-of-mass collision energies well *below* the barrier (1.9 kcal mol⁻¹), we can significantly *suppress* the *adiabatic* (F + H₂) reaction channel, and thereby greatly *enhance* experimental sensitivity for probing *non-adiabatic* (F* + H₂) channels.

The analysis in this paper proceeds in two ways. First, we investigate the total reaction cross-section as a function of center-of-mass collision energy, and then compare these results with adiabatic quantum dynamical calculations^{18,21} on the state-of-the-art F + H₂ potential energy surface. Secondly, we can also exploit the high spectral resolution of the laser based product state detection to maximal advantage, and look for HF(v, J) products that are rigorously inaccessible to adiabatic F + H₂ reactions, but become energetically accessible with the additional ($\Delta E_{\text{spin-orbit}} \approx 1.15$ kcal mol⁻¹²²) spin-orbit excitation along the F* + H₂ path. Most importantly, since the relative energies of the reagents/products are known to high precision from previous spectroscopic studies,^{23,24} this second approach relies solely on conservation of energy and is therefore independent of details of the potential surface such as barrier heights, transition states geometries, tunneling widths, *etc.* The complete center-of-mass collision energy dependence of this reaction will be

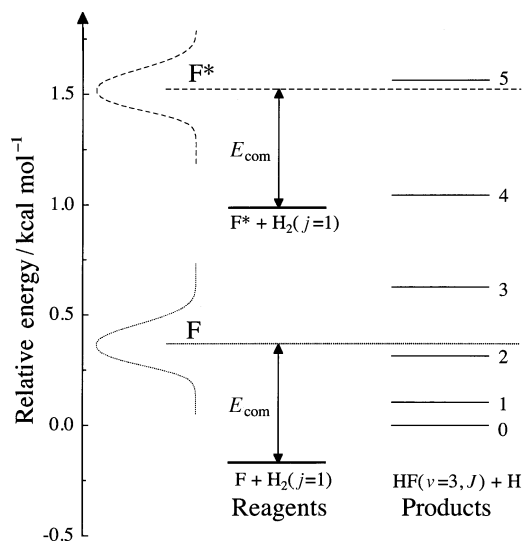


Fig. 1 Simplified energy diagram for the $F(P_{3/2}), F^*(P_{1/2}) + H_2$ reaction at $E_{\text{com}} = 0.54(10)$ kcal mol $^{-1}$ (the curves on the left are the experimental E_{com} distributions). At these low collision energies the range of $HF(v = 3, J)$ levels that can be populated is radically different for F and F^* . For this particular example, the highest energetically allowed state is $HF(v = 3, J = 5)$ for F^* and $HF(v = 3, J = 2)$ for F . Thus, rotationally resolved studies in the $HF(v = 3)$ vibrational manifold provides an unusually sensitive probe of *non-adiabatic* reaction dynamics.

reported elsewhere in greater detail;²⁵ this work focuses explicitly on a few selected collision energies well below the adiabatic $F + H_2$ reaction barrier.

II Experimental

The reactive scattering apparatus used in this work comprises two pulsed molecular jets crossed at right angles ≈ 5 cm downstream from the respective orifices. For the $F + H_2$ experiment, an argon/hydrogen mixture is expanded from the first source through a 145 ± 5 μm pinhole at a total backing pressure of 900 Torr. This corresponds to a measured peak density of $\approx 2 \times 10^{13}$ cm $^{-3}$ in the middle of the intersection region during the 300 μs long pulse duration. Seeding with Ar (0–40%) is used to slow the jet and thereby control the center-of-mass collision energy (E_{com}). The second jet contains F atoms produced in a pulsed mini-slit (300 $\mu\text{m} \times 5$ mm) discharge source.⁶ To achieve the maximal collision energy coverage in the $F + H_2$ experiment ($E_{\text{com}} = 0.3$ –2.4 kcal mol $^{-1}$) two different precursor mixtures are employed, (i) 5% F_2 –95% He, yielding a “fast” F atom jet speed of 1.48 km s $^{-1}$ and (ii) 5% F_2 –20% Ne–75% Ar, yielding a “slow” F atom speed of 0.59 km s $^{-1}$. For the $F + CH_4$ reaction described at the end of this paper, a 10% F_2 –40% Ne–50% Ar mixture is used to obtain “intermediate” F atom speeds of 0.64 km s $^{-1}$. Typical conditions correspond to discharge currents of 100–500 mA at a backing pressure of 30–45 Torr, where the pressures have been optimized for discharge stability. The estimated peak densities (*i.e.*, including carrier gases) are $\leq 5 \times 10^{13}$ cm $^{-3}$ in the intersection region. These backing pressures and densities are chosen to be sufficiently low to ensure reactive/inelastic collision probabilities of less than a few percent per reactant and/or product molecule, which makes the probability of secondary reactions, such as $H + F_2 \rightarrow HF + F$, or rovibrational relaxation of the product, $HF(v, J)$, negligible.

The $HF(v, J)$ products formed in the intersection region are probed *via* direct absorption spectroscopy in a Harriot multipass cell, with a tunable single-mode F-center laser as the IR radiation source. The extremely narrow instrumental resolution (≤ 0.0001 cm $^{-1}$) of the single mode source allows full quantum resolution of the HF product states as well as velocity resolution of ≈ 10 m s $^{-1}$. The transient absorption signal due to $HF(v, J)$ is registered as the difference between signal and reference InSb detectors during the temporal overlap of both gas pulses with the electrical discharge pulse. For each probed $HF(v', J') \leftarrow HF(v'', J'')$ transition, the full Doppler absorbance

profile is recorded (≈ 2500 MHz scans, 3 MHz step size). The profiles can be integrated over the frequency to provide the *absolute* column integrated density differences between upper (v',J') and lower (v'',J'') product states and ultimately analyzed to yield quantum state populations. Averaged over 4–8 pulses, the experimental detection limit for the product HF is estimated to be better than 10^8 molecules cm^{-3} per quantum state.⁶

It is worth noting that the HF absorbances are recorded in *absolute* units, and thus the HF product densities are determined *absolutely*. At present, however, we do not directly probe F atom densities in the intersection zone, and thus all measurements reported are with respect to a reference product state (typically HF($v = 3, J = 1$) measured on $v = 4 \leftarrow 3$ R(1)). This approach yields excellent day-to-day reproducibility and thus also facilitates rigorous comparison over the many days of data collection necessary to extract the full nascent quantum state distributions. Due to the high experimental sensitivity, extremely weak background absorption can sometimes be observed from residual HF impurities in the F₂ discharge. The magnitude of this background HF is quite small ($< 10\%$ of typical peak signals) and can be reliably subtracted by background scans in the absence of the H₂ jet. The reference, probe and background scans are obtained multiple times (typically interleaving five successive scans) under constant F source and H₂ jet conditions to further improve the statistics.

III Results and discussion

Fig. 1 shows a schematic portion of the F + H₂ energy diagram for understanding the essential strategy of this experiment. For simplicity, only the most populated H₂($j = 1$) nuclear spin state is considered, but the principle is identical if H₂($j = 0$) is also included. From bond dissociation energies of HF ($D_0 = 47311(5) \text{ cm}^{-1}$)²⁴ and H₂ ($D_0 = 36118.6(5) \text{ cm}^{-1}$)²³ the F + H₂($j = 1$) reaction exothermicity can be determined with an unusually high precision, $\Delta E = 32.348(14) \text{ kcal mol}^{-1}$. When released in the reaction this energy flows into the relative translation of the H and HF products and into the internal degrees of freedom of HF. The purely rotationless HF($v = 3, J = 0$) state lies very close to the energetic reaction threshold with ground state F atoms, and in fact is only accessible to collisions with F* atoms for $E_{\text{com}} \leq 0.17 \text{ kcal mol}^{-1}$ (Fig. 1). At $E_{\text{com}} \geq 0.17 \text{ kcal mol}^{-1}$, both F and F* reactions can energetically produce HF($v = 3, J$), but with a significantly different range of J levels. For example, at $E_{\text{com}} = 0.54 \text{ kcal mol}^{-1}$ reactions with the ground spin-orbit state F can only produce up to HF($v = 3, J = 2$), whereas spin-orbit excited F* reactions can energetically yield up to HF($v = 3, J = 5$). Thus, studies of quantum state resolved reactive cross-sections into HF($v = 3, J$) under low collision energy conditions can provide an especially sensitive probe for possible *non-adiabatic* (F* + H₂) channels.

With this in mind, the absorption signals out of an HF($v = 3, J$) vibrational manifold have been measured from $E_{\text{com}} \approx 0.3\text{--}2.4 \text{ kcal mol}^{-1}$. Sample raw data representing Doppler profile scans over individual HF rovibrational transitions ($v = 4 \leftarrow 3$; R(0)–R(5)) at $E_{\text{com}} = 2.35 \text{ kcal mol}^{-1}$ and $1.10 \text{ kcal mol}^{-1}$ are shown in Fig. 2. The salient points can be summarized as follows: (i) For a given J level the relative HF($v = 3, J$) transition intensities noticeably decrease, reflecting variation in the corresponding state-to-state reaction cross-sections with E_{com} . (ii) On the other hand, the *shape* of the J distribution is much less sensitive to E_{com} , contrary to what one might anticipate from the F + H₂ reaction energetics (see Fig. 1). It is important to point out that the Doppler profiles for the HF($v = 3, J$) product manifold are largely dominated by angular divergence in the jets, and as a result are independent of both E_{com} and J . This is essentially due to the large mass difference between H and HF products, which deposits most of the excess recoil energy into H atom recoil. Indeed, as confirmed by detailed Monte-Carlo simulations described elsewhere,²⁵ the HF Doppler widths for F + H₂ reactions can be well described by such angular divergence effects. For recoil objects with more comparable masses, such as from F + CH₄ \rightarrow HF + CH₃ reactions, this will of course no longer be true. The different kinematics of such reactions with more than one “heavy” (*i.e.*, non-hydrogenic) atom can therefore lead to a quantum state sensitive Doppler structure in the high resolution absorption profiles, which is briefly addressed at the end of this paper.

The above observations for F + H₂ reactions can be put on a more quantitative basis in the following way. The relative integrated absorbances are first transformed into *column integrated densities*, *i.e.*, $\int [\text{HF}(v, J)] dl$, using known Einstein A coefficients for HF²⁶ as described in ref. 6. This relies on the absence of population in the $v = 4$ manifold, which is energetically inaccessible

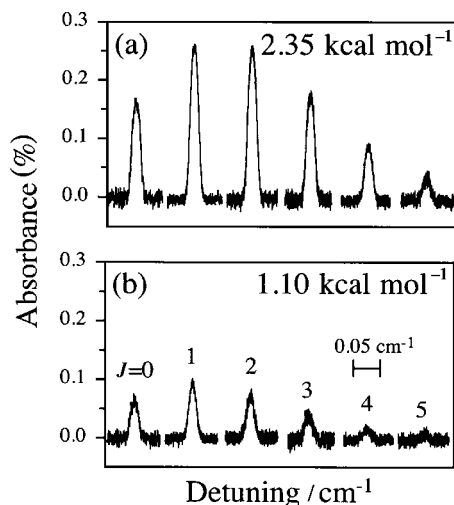


Fig. 2 Sample scans over individual lines of HF in the R-branch of $v = 4 \leftarrow 3$. (a) $E_{\text{com}} = 2.35(46)$ kcal mol $^{-1}$ (b) $E_{\text{com}} = 1.44(24)$ kcal mol $^{-1}$. Note the strong uniform decrease in HF product intensity but rather small shift in product state rotational distributions.

by ≥ 8 kcal mol $^{-1}$ (*i.e.*, to both F and F* reagents) and can be directly tested by $v = 5 \leftarrow 4$ absorption. Previous work⁶ showed that the density to flux transformation for F + H₂ is essentially flat ($\leq 5\%$) due to the favorable “heavy + light-light” reaction kinematics. Thus, the column integrated densities are directly proportional to the state resolved *integrated product fluxes*. The fluxes must scale linearly with the *integrated reaction cross-sections*, densities of both reagents, and relative velocity in the collision. (Note that the last two quantities are both varied in order to tune E_{com} .) Thus, for constant F atom discharge conditions, the relative integrated cross-section into a given final J state can be calculated from

$$\sigma_J(E_{\text{com}}) \propto \frac{\int [\text{HF}(v = 3, J)] dl}{X\sqrt{E_{\text{com}}}} \quad (1)$$

where X is the mole fraction of H₂ in the respective H₂/Ar mixture. The proportionality sign reflects the lack of information on the absolute density of F atoms; all cross-sections are calculated relative to the reference state transition, *i.e.*, for a jet expansion of neat hydrogen ($X = 1$) and $v = 4 \leftarrow 3$ R(1) transition. The data obtained for the “fast” and “slow” fluorine jets are treated independently and then scaled by a single parameter to provide best agreement in the overlapping region of collision energies ($E_{\text{com}} \approx 1.0\text{--}1.7$ kcal mol $^{-1}$).

The dependence of the resulting reaction cross-section on E_{com} is shown in Fig. 3. In the interest of space, only the total (summed over the J states) HF($v = 3$) cross-sections are shown; a complete breakdown by final HF(v, J) rovibrational quantum state, as well as a more detailed comparison with exact quantum calculations, will be presented elsewhere.²⁵ The cross-sections are seen to increase monotonically with E_{com} ; no apparent threshold is observed over this $E_{\text{com}} = 0.3\text{--}2.4$ kcal mol $^{-1}$ range. Even at $E_{\text{com}} = 0.3$ kcal mol $^{-1}$, *i.e.*, the lowest collision energy sampled in the present experiment, the reactive cross-sections for forming HF($v = 3, J$) are still quite appreciable. In fact, the HF($v = 3$) cross-sections at $0.3\text{--}0.9$ kcal mol $^{-1}$ collision energies are down by only ≈ 6 -fold, *i.e.*, considerably higher than one might initially expect for reactions at energies more than a kcal mol $^{-1}$ below the adiabatic (≈ 1.9 kcal mol $^{-1}$) barrier predicted theoretically. This indicates the dramatic importance of quantum tunneling and/or non-adiabatic effects in the F + H₂ reaction dynamics.

This last point becomes particularly clear if the experimental cross-sections are compared with theoretical predictions from “exact” (*i.e.*, fully converged) quantum dynamics calculations on adiabatic potential energy surfaces (PES). Arguably the most rigorous F + H₂ reactive scattering calculations in the energy range of interest have been performed by Castillo *et al.*^{18,21} on the PES of

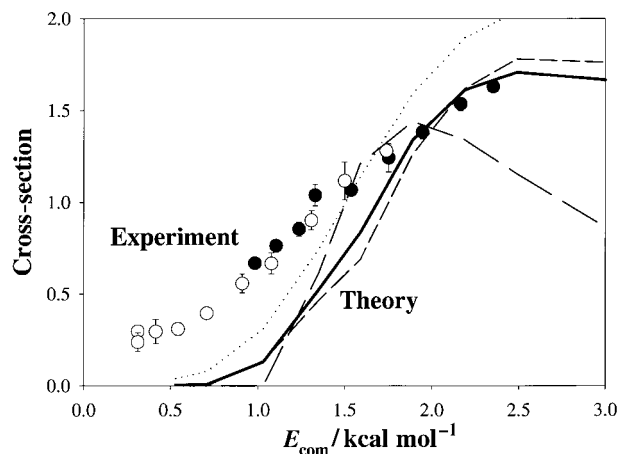


Fig. 3 Total HF($v = 3$) reaction cross-sections as a function of E_{com} . Open and closed circles represent data taken with Ne/F₂ ($v_f \approx 0.59 \text{ km s}^{-1}$) and He/F₂ ($v_f \approx 1.48 \text{ km s}^{-1}$) discharge mixtures, respectively. The theoretical curve is the result of fully converged quantum mechanical scattering calculations on the lowest adiabatic SW PES for $\text{F} + \text{H}_2(j)$: $j = 0$ (long dash); $j = 1$ (short dash); $j = 2$ (dotted); $n\text{-H}_2$ cooled down to 200 K (thick solid line). The E_{com} axis is shifted by $0.38 \text{ kcal mol}^{-1}$ for the theoretical data to reflect spin-orbit effects (see text for details). The vertical axis is dimensionless for the experimental data and is in \AA^2 for the theory. The experimental cross-sections drop off much more slowly with energy than predicted theoretically, consistent with additional contributions from *non-adiabatic* $\text{F}^* + \text{H}_2$ reactions.

Stark and Werner (SW PES),⁷ A more accurate SHW PES, which includes the effects of spin-orbit interaction, is now available¹⁴ but adiabatic calculations on this surface have been performed only for a limited number of energy points.¹⁷ The reaction barrier on the lowest SHW PES is $0.38 \text{ kcal mol}^{-1}$ higher than on the SW PES reflecting lowering the adiabatic $\text{F} + \text{H}_2$ asymptote curve by approximately $1/3\Delta E_{\text{spin-orbit}}$. The shape of the barrier, however, remains essentially unchanged by the inclusion of the spin-orbit effects. The energy dependences of the cross-sections calculated on SW and SHW surfaces are therefore predicted to be quantitatively very similar, apart from a $0.38 \text{ kcal mol}^{-1}$ relative shift in the energy scale.^{17,21,27} Consequently, the extensive calculations on the SW PES are taken as the most reliable theoretical prediction of the *adiabatic* reaction dynamics, simply shifting the E_{com} axis upward by this $0.38 \text{ kcal mol}^{-1}$ spin-orbit induced increase in the barrier height.

Fig. 3 compares the $\text{F} + \text{H}_2(j) \rightarrow \text{HF}(v = 3, \text{ all } J) + \text{H}$ integral reactive cross-sections of Castillo and Manolopoulos²¹ with the experimental results. The theoretical data are presented for H_2 in $j = 0, 1$ and 2 rotational states as well as for $n\text{-H}_2$ at 200 K (*i.e.*, nuclear spin equilibrated at room temperature but cooled rapidly in the jet expansion). The 200 K curve is the most appropriate for comparison with our experiments, since this represents our best rotational temperature estimate for neat H_2 expansions (based on data of refs. 28–31 and on extensive simulations of the experimental Ar/ H_2 jet velocities). The relative experimental cross-sections are scaled overall to match the theoretical $n\text{-H}_2(200 \text{ K})$ data above $E_{\text{com}} = 1.9 \text{ kcal mol}^{-1}$, where the calculations are expected to depend least on transition state geometry, barrier widths, tunneling contributions, *etc.* Note that the theoretical cross-sections decrease significantly more steeply with E_{com} than experimentally observed. Indeed, by $E_{\text{com}} \approx 0.7 \text{ kcal mol}^{-1}$ the theoretical reactivity for 200 K becomes vanishingly small, whereas the experimental cross-sections remain significant down to the lowest measurements at $E_{\text{com}} = 0.31(7) \text{ kcal mol}^{-1}$.

We next consider reasons for this observed discrepancy. The first question is whether theory is performing accurately enough at low E_{com} , which, since the quantum dynamics calculations are numerically exact for a given adiabatic surface, relies on the quality of the potential surface. Indeed, until the present work, the $\text{F} + \text{H}_2$ calculations have only been tested against extensive molecular beam studies at $E_{\text{com}} \geq 1.84 \text{ kcal mol}^{-1}$.^{3,16–18,32} A closely related issue is that the SHW PES is known to *underestimate* the global reaction exothermicity by $\approx 0.2 \text{ kcal mol}^{-1}$, which would be expected to influence these calculations most at low E_{com} . The effect of such

asymptotic potential surface errors on the reaction cross-sections is difficult to estimate, and depends on where this 0.2 kcal mol⁻¹ difference accrues. For example, a 0.2 kcal mol⁻¹ error is localized in the exit channel would have a negligible effect on the energy dependent cross-sections, whereas if it were localized in the entrance channel, the cross-sections for forming HF(*v* = 3) would have the same shape as in Fig. 3, only shifted down by 0.2 kcal mol⁻¹ along the E_{com} axis. However, even such a shift would fail to bring the experiment and theory in agreement, the latter still severely underestimating the reaction cross-sections at low E_{com} . Thus, though potential surface errors in the asymptotic exothermicity may have some effect, it is not likely to be the main contributor to the underpredicted cross-sections observed experimentally.

The possibility that the enhanced reactivity at low E_{com} is due to rotationally hot H₂ (*i.e.*, $j > 1$) also does not agree with the observations. First, rotational excitation of H₂ is predicted to have only a small influence on the reaction cross-sections,^{33,34} as explicitly confirmed by the calculations of Castillo and Manolopoulos. Secondly, a rotational temperature of $T_{\text{rot}} < 200$ K for the H₂ jets is a realistic upper limit (lower for H₂ jets seeded with Ar), with completely negligible rotational heating of H₂ due to collisions on the way to the intersection region. Though the reaction threshold shifts to lower E_{com} for higher j , the calculated F + H₂($j = 2$) cross-sections below 1 kcal mol⁻¹ are still far too small to account for the experimental observation. In fact, even theoretical predictions for a jet of “neat” H₂($j = 2$) would still qualitatively fail to reproduce the experimental cross-sections.

The most credible explanation of the enhanced reactivity at low E_{com} is *via* non-adiabatic reaction of F* with H₂. The spin-orbit excited F* atoms produced in the discharge carry $\Delta E_{\text{spin-orbit}} = 1.15$ kcal mol⁻¹ internal energy compared to F and can energetically produce HF($v = 3, J = 0$) even at $E_{\text{com}} = 0$ (Fig. 1). The most compelling evidence in favor of this hypothesis comes from observation of HF($v = 3, J$) product states which can only be accessed energetically *via* the *non-adiabatic* F* + H₂($j = 0, 1$) channel. The essential idea in this analysis is based on simple energy conservation arguments. The exothermicity of the F + H₂ reaction is known very accurately from spectroscopic measurements;^{23,24} $\Delta E = 32.001(14)$ and $32.348(14)$ kcal mol⁻¹ for reactions F + H₂($j = 0$) and F + H₂($j = 1$), respectively. Furthermore, the H atom product can only be in the (¹S) ground state, which means that this excess energy must be converted into either (i) internal rotation and vibration of the HF(v, J) or (ii) relative recoil kinetic energy (E_{recoil}) of the H + HF products in the center of mass frame. Thus, $E_{\text{HF}(v,J)} + E_{\text{recoil}} = E_{\text{com}} + \Delta E$, which because E_{recoil} must be non-negative leads to a *rigorous upper limit* on the HF internal state energy of $\{E_{\text{HF}(v,J)}\}_{\text{max}} = E_{\text{com}} + \Delta E$ for a given initial state of F/H₂ reagents and a known center-of-mass collision energy.

By way of testing this idea, Fig. 4 displays the final quantum state resolved HF($v = 3, J$) reaction cross-sections for $E_{\text{com}} = 0.54(10)$ kcal mol⁻¹. The distributions are plotted as a function of the threshold energy ($E_{\text{thr}} = E_{\text{HF}(v,J)} - \Delta E_{j=1}$), which is the minimal collision energy required to make the process F + H₂($j = 1$) → HF($v = 3, J$) + H energetically accessible. States with $E_{\text{thr}} > E_{\text{com}}$ are rigorously closed for the ground state F reaction and can only be produced from the non-adiabatic channel. The distributions of E_{com} in the jet intersection region (obtained from extensive high resolution Dopplerimetry and Monte-Carlo simulations described elsewhere²⁵) are also shown in the figure. The data at $E_{\text{com}} = 0.54(10)$ kcal mol⁻¹ clearly indicate *three* HF($v = 3, J$) states (*i.e.*, $J = 3, 4$ and 5) experimentally observed in these distributions that are energetically inconsistent with the *adiabatic* F + H₂($j = 1$) reactions and only become energetically accessible by *non-adiabatic* channels built on F* + H₂($j = 1$).

Such non-adiabatic effects in the F + H₂ reaction have proven elusive to detect in previous crossed beam experiments. Indeed, the only previous report of a non-adiabatic reaction channel prior to this work was in studies of the F + D₂ reaction by Faubel and coworkers,³⁵ where a peak in the DF product TOF spectra was observed at arrival times consistent with F* + D₂ energetics.³⁵ Somewhat surprisingly, recent crossed beam studies in F + H₂ collisions by these same workers did not reveal inelastic E–T or near-resonant E–R energy exchange in F*/F + H₂ collisions,³⁶ which might be expected to be have comparable cross-sections to H atom abstraction.³ In this regard, it is important to note that the current studies are based on threshold phenomena and are performed at collision energies significantly *below* the adiabatic reaction barrier, as well as at much lower energies than previously investigated. In conjunction with complete quantum state resolution of the final product states offered by IR laser detection, this near threshold mode of

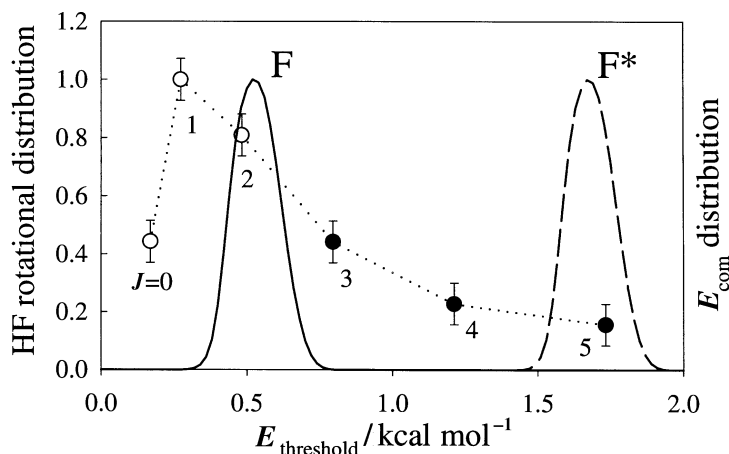


Fig. 4 Rotational populations of HF($v = 3, J$) observed at $E_{\text{com}} = 0.54(10)$ kcal mol $^{-1}$ vs. threshold collision energy required to produce a given J state from the F + H $_2$ ($j = 1$) reaction. The smooth Gaussian-like curves are the distributions of energy available from F + H $_2$ ($j = 1$) (solid line) and F* + H $_2$ ($j = 1$) (dashed line) reactions. All shaded J states are energetically closed for F + H $_2$ ($j = 1$) and can only be produced from the F* + H $_2$ non-adiabatic channel.

operation allows one to selectively *suppress* the adiabatic reaction pathways (*i.e.*, by looking below the barrier or at states energetically inaccessible to F + H $_2$). This leads to a corresponding enhancement in experimental sensitivity for *non-adiabatic* pathways that makes them much easier to isolate and detect than in the competing presence of conventional adiabatic channels.

By way of contrast, many theoretical studies have predicted sizable non-adiabatic effects in the F + H $_2$ reaction (see ref. 3 and references therein). However, it has been extremely challenging to incorporate these non-adiabatic effects rigorously in a full multisurface calculation. It is therefore noteworthy that Alexander *et al.*²⁷ have recently succeeded in performing full quantum reactive scattering calculations for F + H $_2$ including all three SHW PES, Born–Oppenheimer derivative coupling, spin–orbit and Coriolis coupling effects. These results predict significant reaction probability for the non-adiabatic F* + H $_2$ channel into HF($v = 3, J$) + H, specifically on the order of 10% of the adiabatic F + H $_2$ channel at near and above threshold energies ($E_{\text{com}} \approx 2$ kcal mol $^{-1}$). Even more importantly, the calculated non-adiabatic cross-sections for reactive scattering to form HF($v = 3, J$) decrease much more slowly with E_{com} than the adiabatic ones and therefore dominate the reaction at low collision energies, *i.e.*, in qualitative agreement with the present experimental observations. Indeed, these full surface calculations indicate that below $E_{\text{com}} \approx 0.75$ kcal mol $^{-1}$, essentially all HF(v, J) products in the $v = 3$ manifold arise from the non-adiabatic F* + H $_2$ ($j = 1$) channel. Even with a maximum possible shift in these predictions due to ≈ 0.2 kcal mol $^{-1}$ asymptotic errors in the potential, this would still imply that the product state distributions in Fig. 4 at $E_{\text{com}} = 0.54$ kcal mol $^{-1}$ reflect very substantial contributions from non-adiabatic F* + H $_2$ reaction pathways. One important caveat in these predictions is that multisurface calculations have only been successfully performed for the lowest partial wave (*i.e.*, $J_{\text{tot}} = 1/2$) and are not yet converged with respect to total angular momentum. It will be therefore be quite interesting to see the results of fully converged calculations, as well as the threshold dynamical behaviors predicted for reaction of F, F* and H $_2$ ($j = 0, 1, 2$) into each final HF(v, J) state for the most rigorous comparison with the current experimental data.

IV Velocity distributions from high resolution IR laser dopplerimetry

As a final comment, we turn to a discussion of further potential applications of high resolution direct absorption methods in the crossed jet apparatus. Specifically, the $\Delta\nu = 0.0001$ cm $^{-1}$ resolution of Doppler absorbance profiles probes quantum state resolved velocity distributions along the laser detection axis, which can also be used to extract information on *state-to-state differential cross-sections*. This is currently difficult for us to detect in the F + H $_2$ reaction for

unskimmed jets, since the vast majority of the excess recoil energy appears in the light H atom and not the heavy HF product. However, for other H atom abstraction reactions, such as $F + CH_4 \rightarrow HF + CH_3$, the product masses are more equally balanced, thus providing a much stronger “kick” on the recoiling HF product. We thus conclude this paper with preliminary Dopplerimetry data on quantum state resolved velocity distributions from reactions of $F + CH_4$.

An example of a typical Doppler profile is given in Fig. 5 which displays the $v = 3 \leftarrow 2$ P(2) transition of HF produced in the jet intersection region at $E_{\text{com}} = 1.7(5)$ kcal mol⁻¹. Both the upper HF($v' = 3, J' = 1$) and lower HF($v'' = 2, J'' = 2$) states connected by the transition are populated by the reaction, each characterized by its own angular and product speed distribution. Due to the high spectral resolution of the laser, each frequency detuning corresponds uniquely to a certain projection of HF velocity onto the laser axis. In this particular case the population is inverted ($[HF]' > [HF]''$) for the molecules moving in the *low* velocity subgroup leading to net stimulated *emission* rather than *absorption* in the center of the profile. The situation changes dramatically at larger frequency detuning (corresponding to recoil velocities of $\approx 1.3 \times 10^5$ cm s⁻¹). With a maximum recoil energy (E_{recoil}) of ≈ 1 kcal mol⁻¹ available, the HF($v' = 3, J' = 1$) products do not have enough available energy to acquire such a velocity. On the other hand, up to ≈ 10 kcal mol⁻¹ of energy is in principle available for relative HF/CH₃ translation in the $v = 2$ manifold (depending on the internal state of the methyl radical) permitting the HF($v = 2$) product to be considerably speedier. As a result, for this velocity subgroup only the lower state is populated and the signal becomes purely absorptive. We note that similar absorption/stimulated emission Doppler spectral signatures were also observed and reported for our previous studies of $F + H_2$ reactive scattering,⁶ but due to smaller HF recoil speeds and lower signal to noise, the effects were much more subtle.

In order to isolate the velocity distribution for individual rovibrational states the data are analyzed as follows. Since the upper $v = 4$ state is far above the energetic reaction limit, the HF($v = 3, J$) velocity distributions can be directly determined from the set of $v = 4 \leftarrow 3$ Doppler profiles. The HF($v = 2, J$) distributions are then obtained from the compound Doppler profiles connecting the $v = 2$ and $v = 3$ states like the one shown in Fig. 5. The velocity distributions for each lower HF state of interest can be obtained by successively working down the vibrational manifold. The resulting distributions can then be modeled to infer the product angular distribution in the center-of-mass frame, using a singular value decomposition strategy similar to that previously demonstrated for HF + Ar inelastic scattering.^{3,7} Briefly, the center-of-mass scattering angle θ_{com} is divided into bins of equal $\cos(\theta_{\text{com}})$ increments. For scattering into each angular bin a model Doppler profile (“basis function”) is predicted from a detailed Monte-Carlo integration of

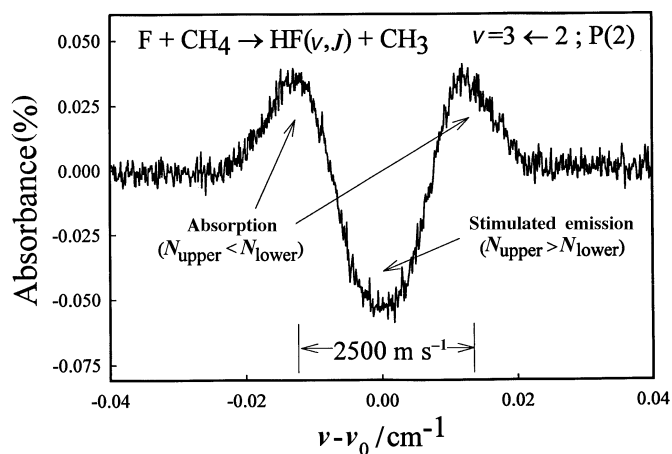


Fig. 5 A sample high resolution scan over the $v = 3 \leftarrow 2$ P(2) transition from nascent HF($v'' = 2, J'' = 2$) formed by reactive scattering of $F + CH_4$. The Doppler profile is determined by the relative densities and velocity distributions of the HF($v'' = 2, J'' = 2$) and HF($v' = 3, J' = 1$) states in the jet intersection zone and carries information about the center-of-mass angular distribution of the nascent HF.

the appropriate experimental conditions. The experimental Doppler profile is then least-squares fitted to a linear combination of the model “basis functions”, with coefficients corresponding to relative weights in the product angular distribution.

A complete data analysis is currently underway³⁸ but a few trends are already clear from fits for the most populated HF($v = 2$) manifold. (i) A major fraction of the exothermicity goes into internal rovibrational energy of the HF(v, J) product. (ii) For all but the highest vibrational manifold of product HF($v = 3$), the recoil kinetic energy between the HF and CH₃ fragments represents the next largest energy sink. (iii) The HF($v = 2$) products appear to be predominantly scattered in the *backward/forward vs.* sideward direction. (iv) A relatively minor fraction of the excess energy goes into internal energy of the CH₃ fragments. This is consistent with the results of Sugawara *et al.*³⁹ who demonstrated that the CH₃ product is relatively unexcited both rotationally ($T_{\text{rot}} \approx 300$ K) and vibrationally ($T_{\text{vib}} \approx 1000$ K in the umbrella mode). To the best of our knowledge, no reaction differential cross-section studies have been reported for F + CH₄, which makes the present Dopplerimetry results particularly valuable. Unfortunately, theoretical data for the reaction are still rather scarce,^{40–42} which precludes a more rigorous, direct comparison between experiment and theory. It is our hope that such results on product state and velocity distributions in F + CH₄ (and other systems such as F + H₂O) will provide the necessary stimulus to both the *ab initio* and quantum dynamics community for further studies of atom + polyatomic reaction dynamics at the fully quantum state-to-state level.

V Summary

High resolution IR direct absorption spectroscopy is applied to study the dynamics of hydrogen-abstraction reactions by F atoms from H₂ and CH₄ under single collision conditions in a crossed supersonic jet apparatus. Rovibrationally resolved cross-sections for the F + H₂ → HF($v = 3, J$) + H reaction have been observed as a function of E_{com} for several energies *below* the 1.9 kcal mol⁻¹ adiabatic barrier for reactions of ground spin-orbit F with n -H₂. The cross-sections are compared with exact quantum dynamics calculations^{21,27} on the recent fully *ab initio* potential energy surface.^{7,14} Theoretical cross-sections decrease rapidly with E_{com} below the barrier, essentially vanishing by $E_{\text{com}} \approx 0.7$ kcal mol⁻¹. Experimental cross-sections drop off more slowly with E_{com} , and are still measurable at the lowest center-of-mass energies sampled ($E_{\text{com}} \approx 0.3$ kcal mol⁻¹). Furthermore, several additional product rotational states in HF($v = 3, J$) are observed that are energetically inaccessible at a given E_{com} from adiabatic reactions with ground spin-orbit F atoms with n -H₂ ($j = 0, 1$). This latter observation is especially informative, since it depends only on the *asymptotic* properties of the potential surface, well characterized by previous spectroscopic studies. These observations are most convincingly explained by contributions from non-adiabatic F*(²P_{1/2}) + n -H₂ channels, which have been selectively enhanced in these studies by operation at collision energies significantly *below* the adiabatic reaction barrier theoretically predicted for F(²P_{3/2}) + n -H₂. Preliminary results on the crossed jet reactions between F + CH₄ are also reported, which successfully demonstrate that HF(v, J) *velocity* distributions can be obtained in state-to-state reactive scattering *via* high-resolution direct absorption measurements.

Acknowledgements

This work has been supported by grants from the Air Force Office of Scientific Research and the National Science Foundation. We are indebted to J. Castillo and D. Manolopoulos for sharing their calculations with us prior to publication, as well as many stimulating discussions.

References

- 1 H. Shafer III, *J. Phys. Chem.*, 1985, **89**, 5336.
- 2 J. C. Polanyi and J. L. Schreiber, *Faraday Discuss. Chem. Soc.*, 1977, **62**, 267.
- 3 D. Manolopoulos, *J. Chem. Soc., Faraday Trans.*, 1997, **93**, 673.
- 4 J. Anderson, *Adv. Chem. Phys.*, 1980, **41**, 229.
- 5 L. J. Butler, *Annu. Rev. Phys. Chem.*, 1998, **49**, 125.
- 6 W. B. Chapman, Jr., B. W. Blackmon, S. Nizkorodov and D. J. Nesbitt, *J. Chem. Phys.*, 1998, **109**, 9306.
- 7 K. Stark and H. Werner, *J. Chem. Phys.*, 1996, **104**, 6515.

- 8 R. D. Coombe and G. C. Pimentel, *J. Chem. Phys.*, 1973, **59**, 251.
- 9 S. Lu, C. Liu, X. Yang, K. Li, Y. Gu and Y. Tao, *J. Chem. Phys.*, 1988, **88**, 2379.
- 10 D. M. Neumark, A. M. Wodtke, G. N. Robinson, C. C. Hayden and Y. T. Lee, *J. Chem. Phys.*, 1985, **82**, 3045.
- 11 N. Jonathan, C. M. Mellier-Smith and D. H. Slater, *Mol. Phys.*, 1971, **20**, 93.
- 12 D. Truhlar, *J. Chem. Phys.*, 1972, **56**, 3189.
- 13 J. T. Muckerman and M. D. Newton, *J. Chem. Phys.*, 1972, **56**, 3191.
- 14 B. Hartke and H. Werner, *Chem. Phys. Lett.*, 1997, **280**, 430.
- 15 G. Dharmasena, K. Copeland, J. Young, R. Lasell, T. Phillips, G. Parker and M. Keil, *J. Phys. Chem. A*, 1997, **101**, 6429.
- 16 F. Aoiz, L. Banares, B. MartinezHaya, J. Castillo, D. Manolopoulos, K. Stark and H. Werner, *J. Phys. Chem. A*, 1997, **101**, 6403.
- 17 J. F. Castillo, B. Hartke, H. J. Werner, F. J. Aoiz, L. Banares and B. Martinez-Haya, *J. Chem. Phys.*, 1998, **109**, 7224.
- 18 J. Castillo, D. Manolopoulos, K. Stark and H. Werner, *J. Chem. Phys.*, 1996, **104**, 6531.
- 19 E. Rosenman and A. Persky, *Chem. Phys.*, 1995, **195**, 291.
- 20 F. Aoiz, L. Banares, V. Herrero, K. Stark and H. Werner, *Chem. Phys. Lett.*, 1996, **254**, 341.
- 21 J. Castillo and D. Manolopoulos, personal communications.
- 22 *JANAF Thermochemical Tables*, NSRDS-NBS 37, 2nd edn., 1971.
- 23 W. C. Stwalley, *Chem. Phys. Lett.*, 1970, **6**, 241.
- 24 W. T. Zemke, W. C. Stwalley, J. A. Coxon and P. G. Hajigeorgiou, *Chem. Phys. Lett.*, 1991, **177**, 412.
- 25 S. A. Nizkorodov, W. W. Harper, W. B. Chapman, Jr., B. W. Blackmon and D. J. Nesbitt, *J. Chem. Phys.*, submitted.
- 26 E. Arunan, D. W. Setset and J. F. Ogilvie, *J. Chem. Phys.*, 1992, **97**, 1734.
- 27 M. Alexander, H. Werner and D. Manolopoulos, *J. Chem. Phys.*, 1998, **109**, 5710.
- 28 J. E. Pollard, D. J. Trevor, T. T. Lee and D. A. Shirley, *J. Chem. Phys.*, 1982, **77**, 4818.
- 29 P. Huber-Walchli and J. W. Nibler, *J. Chem. Phys.*, 1982, **76**, 273.
- 30 R. J. Gallagher and J. B. Fenn, *J. Chem. Phys.*, 1974, **60**, 3492.
- 31 K. Dharmasena, J. Jefferies, G. Mu, J. Young, B. Bergeron, R. Littell and N. Shafer-Ray, *Rev. Sci. Instrum.*, 1998, **69**, 2888.
- 32 M. Baer, M. Faubel, B. Martinez-Haya, L. Rusin, U. Tappe and J. Toennies, *J. Chem. Phys.*, 1998, **108**, 9694.
- 33 J. Harrison, L. Isakson and H. Mayne, *J. Chem. Phys.*, 1989, **91**, 6906.
- 34 J. B. Song and E. A. Gislason, *J. Chem. Phys.*, 1995, **103**, 8884.
- 35 M. Faubel, B. Martinezhaya, L. Rusin, U. Tappe and J. Toennies, *Z. Phys. Chem.*, 1995, **188**, 197.
- 36 M. Faubel, L. Rusin, S. Schlemmer, F. Sonderrmann, U. Tappe and J. Toennies, *J. Chem. Soc., Faraday Trans.*, 1993, **89**, 1475.
- 37 W. Chapman, M. Weida and D. Nesbitt, *J. Chem. Phys.*, 1997, **106**, 2248.
- 38 W. W. Harper, S. A. Nizkorodov and D. J. Nesbitt, *J. Chem. Phys.*, in preparation.
- 39 K. Sugawara, F. Ito, T. Nakanaga, H. Takeo and C. Matsumura, *J. Chem. Phys.*, 1990, **92**, 5328.
- 40 A. Gauss, Jr., *J. Chem. Phys.*, 1976, **65**, 4365.
- 41 J. C. Corchado and J. S. Espinosa-Garcia, *J. Chem. Phys.*, 1996, **105**, 3160.
- 42 H. Kornweitz, A. Persky and R. D. Levine, *Chem. Phys. Lett.*, 1998, **289**, 125.

Paper 9/01824G